

Real-time magnetic resonance imaging of deep venous flow during muscular exercise – preliminary experience

Arun Antony Joseph^{1,2}, Klaus-Dietmar Merboldt¹, Dirk Voit¹, Johannes Dahm³, Jens Frahm^{1,2}

¹Biomedizinische NMR Forschungs GmbH, Max Planck Institute for Biophysical Chemistry, Göttingen, Germany; ²DZHK, German Center for Cardiovascular Research, partner site Göttingen, Germany; ³Herz & Gefäßzentrum Göttingen am Krankenhaus Neu-Bethlehem, Göttingen, Germany

Contributions: (I) Conception and design: AA Joseph, KD Merboldt, D Voit, J Frahm; (II) Administrative support: J Frahm; (III) Provision of study material or patients: J Dahm; (IV) Collection and assembly of data: AA Joseph, KD Merboldt; (V) Data analysis and interpretations: AA Joseph, KD Merboldt, J Frahm; (VI) Manuscript writing: All authors; (VII) Final approval of manuscript: All authors.

Correspondence to: Dr. Arun A. Joseph. Biomedizinische NMR Forschungs GmbH, Max Planck Institute for Biophysical Chemistry, 37070 Göttingen, Germany. Email: ajoseph@mpibpc.mpg.de.

Background: The accurate assessment of peripheral venous flow is important for the early diagnosis and treatment of disorders such as deep-vein thrombosis (DVT) which is a major cause of post-thrombotic syndrome or even death due to pulmonary embolism. The aim of this work is to quantitatively determine blood flow in deep veins during rest and muscular exercise using a novel real-time magnetic resonance imaging (MRI) method for velocity-encoded phase-contrast (PC) MRI at high spatiotemporal resolution.

Methods: Real-time PC MRI of eight healthy volunteers and one patient was performed at 3 Tesla (Prisma fit, Siemens, Erlangen, Germany) using a flexible 16-channel receive coil (Variety, NORAS, Hoechberg, Germany). Acquisitions were based on a highly undersampled radial FLASH sequence with image reconstruction by regularized nonlinear inversion at $0.5 \times 0.5 \times 6 \text{ mm}^3$ spatial resolution and 100 ms temporal resolution. Flow was assessed in two cross-sections of the lower leg at the level of the calf muscle and knee using a protocol of 10 s rest, 20 s flexion and extension of the foot, and 10 s rest. Quantitative analyses included through-plane flow in the right posterior tibial, right peroneal and popliteal vein (PC maps) as well as signal intensity changes due to flow and muscle movements (corresponding magnitude images).

Results: Real-time PC MRI successfully monitored the dynamics of venous flow at high spatiotemporal resolution and clearly demonstrated increased flow in deep veins in response to flexion and extension of the foot. In normal subjects, the maximum velocity (averaged across vessel lumen) during exercise was $9.4 \pm 5.7 \text{ cm}\cdot\text{s}^{-1}$ for the right peroneal vein, $8.5 \pm 4.6 \text{ cm}\cdot\text{s}^{-1}$ for the right posterior tibial vein and $17.8 \pm 5.8 \text{ cm}\cdot\text{s}^{-1}$ for the popliteal vein. The integrated flow volume per exercise (20 s) was 1.9, 1.6 and 50 mL (mean across subjects) for right peroneal, right posterior tibial and popliteal vein, respectively. A patient with DVT presented with peak flow velocities of only about $2 \text{ cm}\cdot\text{s}^{-1}$ during exercise and less than $1 \text{ cm}\cdot\text{s}^{-1}$ during rest.

Conclusions: Real-time PC MRI emerges as a new tool for quantifying the dynamics of muscle-induced flow in deep veins. The method provides both signal intensity changes and velocity information for the assessment of blood flow and muscle movements. It now warrants extended clinical trials to patients with suspected thrombosis.

Keywords: Deep venous flow; real-time MRI; phase-contrast MRI

Submitted Jun 30, 2016. Accepted for publication Sep 19, 2016.

doi: 10.21037/cdt.2016.11.02

View this article at: <http://dx.doi.org/10.21037/cdt.2016.11.02>

Introduction

Deep-vein thrombosis (DVT) is an important area of research as it is a major cause of post-thrombotic syndrome or even death due to pulmonary embolism (1-3). A diagnosis at an early stage may save lives through focused therapy. Although contrast venography has been considered as the gold standard for the diagnosis of DVT (4), it is invasive and requires contrast media. Presently, duplex and compression ultrasonography is the preferred technique to image flow in the proximal veins of the lower leg (5). It combines morphological (e.g., thrombus) and functional aspects (e.g., venous flow) with a functional stress test such as gentle pressure on the veins (i.e., compression). Further advantages are widespread availability and cost efficacy. However, its applicability to small deep veins is hampered by the presence of bones, muscles and soft tissues which affect the quality of ultrasound signal recording (6,7). Ultrasound measurements are operator dependent and lack standardized protocols for obtaining blood vessel diameter, lumen or quantitative flow measurements, in particular in pathologic anatomies like post-thrombotic syndromes or varicose veins.

Magnetic resonance imaging (MRI) has also been used to measure flow through velocity-encoded phase-contrast (PC) techniques (8-10). The method requires two acquisitions with velocity-compensated and velocity-encoding gradients to assess through-plane flow perpendicular to the imaging section. A subsequent phase difference operation of the two complex images provides a T1-weighted magnitude image of the anatomy and a PC velocity map of moving or flowing signals. Although PC MRI has recently been combined with parallel imaging (11,12) and non-Cartesian acquisition schemes (13,14) to reduce acquisition times, most of these techniques still rely on ECG-gating and the underlying assumption of cardiac periodicity (15) which precludes the application to non-cardiac related flow. In contrast, real-time flow MRI techniques promise flow information of arbitrary dynamic processes (16-18). Unfortunately, these early studies sacrificed spatial resolution to achieve sufficient temporal resolution and therefore were unable to monitor flow in small blood vessels such as the veins of the lower leg. Most recently, real-time MRI using highly undersampled radial FLASH with image reconstruction by regularized nonlinear inversion (NLINV) has been developed to provide images at both high spatial and temporal resolution (19-21). This technique has further been extended to

quantitatively image through-plane flow in real time (22-24) and successfully been applied to a number of clinical scenarios (25-27). The aim of this study was to explore the potential of real-time PC MRI to assess deep venous flow at high spatial and temporal resolution in normal subjects.

Methods

Subjects and MRI

Flow MRI was performed at 3 Tesla (Prisma fit, Siemens Healthcare, Erlangen, Germany) with use of a 16-channel receive coil (Variety, NORAS, Hoechberg, Germany). The coil consists of two very flexible 8-channel elements which were easily wrapped around the subjects lower leg. They are specially designed to study smaller objects at excellent signal-to-noise ratio compared to the standard coils of the MRI vendor.

A group of eight healthy volunteers (age 25–62 years) with no known illness and a patient with DVT (total occlusion) in the popliteal vein (confirmed by duplex-ultrasound) were recruited after approval by the institutional review board of the University Medical Center Göttingen. All participants gave written informed consent before MRI. Subjects were studied in supine position with a feet-first position inside the scanner. A protocol of muscular exercise was visually projected to the subjects during real-time MRI. While the protocol for healthy volunteers consisted of an initial rest phase of 10 s, foot flapping of 20 s and another rest phase of 10 s, the patient started with a rest phase of 16 s followed by a foot flapping phase of 24 s to better detect residual flow during compromised muscle performance. During foot flapping, the subjects were asked to perform flexion and extension of the foot in an alternating fashion without specific instructions about the frequency. Flow measurements were performed in two cross-sections of the leg at about the mid-region of the calf muscle and close to the knee. The total examination time per subject in the scanner was about 30 min.

Real-time PC MRI

Real-time PC MRI was performed using highly undersampled radial FLASH with image reconstruction by regularized nonlinear inversion (NLINV) as previously described (24). The scan parameters for the measurement were: in-plane resolution $0.5 \times 0.5 \text{ mm}^2$, field of view $128 \times 128 \text{ mm}^2$, matrix size 256×256 pixels, repetition time

(TR) 4.55 ms, echo time (TE) 3.05 ms, flip angle 12°, slice thickness 6 mm. The two velocity-encoded real-time acquisitions each employed 11 radial spokes and resulted in a temporal resolution of 100 ms for the acquisition of both datasets, i.e., 10 frames per second (fps) per PC map. The velocity sensitivity (VENC) was adjusted to a value between 80 and 95 cm·s⁻¹ to avoid phase wrapping for arterial blood flow.

Online reconstruction of real-time images was achieved by running a parallelized version of the NLINV algorithm on a bypass computer (sysGen/TYAN Octuple-GPU, Sysgen, Bremen, Germany) equipped with two processors (CPUs, Sandy Bridge E5-2650, Intel, Santa Clara, CA, USA) and eight graphics processing units (TITAN, NVIDIA, Santa Clara, CA, USA) (28). The system is fully integrated into the reconstruction pipeline of the commercial MRI system. The reconstruction speed for the setting used here was 5.2 fps for both the magnitude images and PC maps.

Image evaluation

Quantitative analyses of magnitude images and PC maps relied on CAIPI prototype software (Fraunhofer MEVIS, Bremen, Germany) especially developed to deal with real-time MRI data (29). This software accomplishes fully automated vessel segmentation and flow analyses of real-time PC MRI data throughout entire time series (here: 40 s duration = 400 magnitude images and 400 PC maps). The program works without the need for manual corrections as any displacement of a vessel is taken care of by the segmentation algorithm. Flow parameters included velocities averaged across the respective vessel lumen and corresponding flow volumes. In addition, signal intensity variations in the T1-weighted magnitude images (veins and muscles) were determined because of their high sensitivity to very small through-plane motions as recently demonstrated for real-time flow MRI of the cerebrospinal fluid (26).

Results

As shown in *Figure 1*, real-time PC MRI provides high-resolution magnitude images and PC velocity maps which allow for a proper delineation of the right posterior tibial vein, right peroneal vein, and popliteal vein at two different positions of the lower leg. These vessels were seen in all subjects and therefore chosen for analysis, while two

peroneal or posterior tibial veins were detected in only a few cases. During exercise, the method yields quantitative information about the performance of the gastrocnemius muscle which influences the venous flow. In PC velocity maps, venous and arterial flow are represented as white and black signal, respectively, in accordance to their respective upward and downward direction of flow.

Figure 2 depicts time courses of the mean velocities of the gastrocnemius muscle and peroneal artery as well as of the right peroneal and posterior tibial vein in response to exercise at the level of the calf muscle. It is clearly seen that deep venous flow in the lower leg (*Figure 2C,D*) almost exclusively occurs during muscle movement, i.e., synchronous to the contraction (forward and backward velocity) of the gastrocnemius muscle during foot flapping. This is accompanied by an increased flow velocity in the peroneal artery.

Figure 3 shows the mean velocities and corresponding signal intensities of the gastrocnemius medial head muscle and popliteal vein at about the lower knee. Similar to the veins in the calf muscle, also flow in the popliteal vein is largely dependent on muscular contractions. Its mean velocity is generally higher than that of the peroneal and posterior tibial veins. Again synchronous to the muscle-induced velocities, signal intensity changes in the corresponding magnitude images are most sensitive to qualitatively indicate the presence of inflow or through-plane motion. This is because the contrast-to-noise ratio of the flow-related signal change is usually better than that of the corresponding velocity change (26).

Table 1 summarizes the exercise-induced maximal velocities in deep veins obtained during foot flapping for all subjects (mean and SD during the exercise phase). These flow velocities across subjects were about 8 to 10 cm·s⁻¹ in the right peroneal and posterior tibial vein and almost twice as high in the popliteal vein, respectively. The observation of large variations in this group of healthy volunteers most likely reflects individual differences in muscular performance. Similarly, *Table 2* shows the net volume of upward flow towards the heart in deep veins. The values represent the integrated response to multiple foot flaps during the 20 s period of exercise. Mean values across subjects were only up to 2 mL for the right peroneal and posterior tibial vein, whereas the net flow volume in the popliteal vein of 50 mL (i.e., approximately 4 to 5 mL per foot flap) results from the accumulation of venous return from the lower leg which leads to a larger diameter and higher flow velocity.

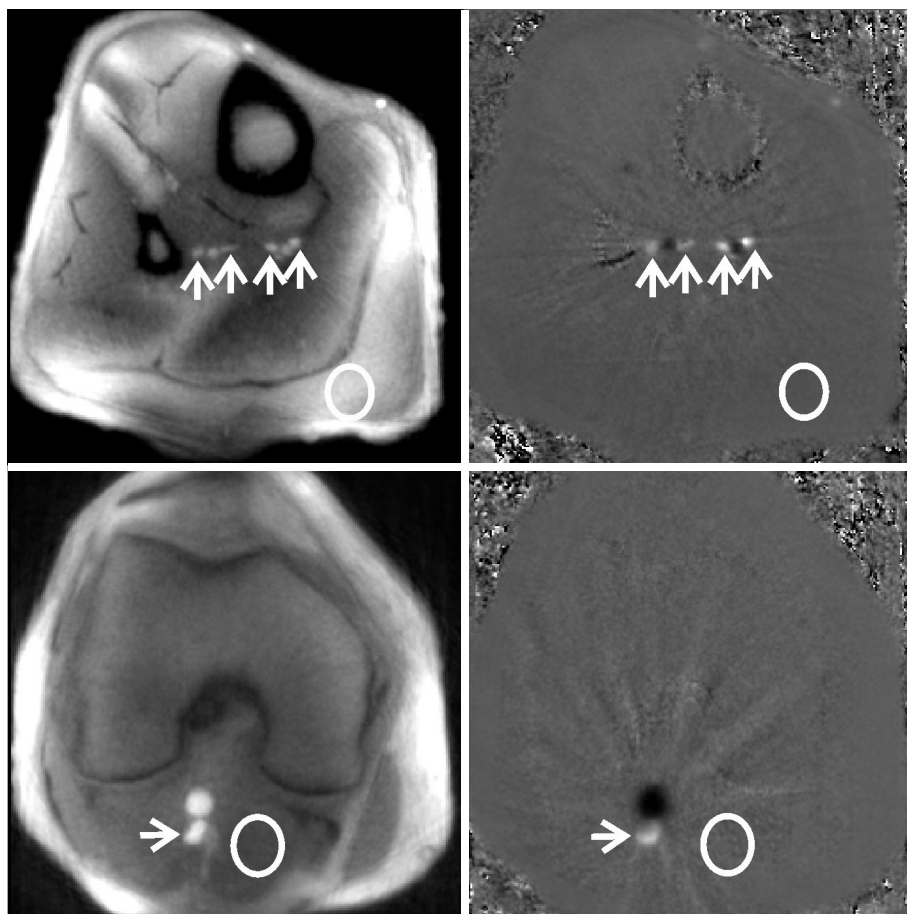


Figure 1 Selected real-time T1-weighted images and PC maps of deep venous flow (bright signal in PC maps = upward flow) during muscle movement (subject #5). (Top) At the level of the calf muscle: arrows from left to right refer to the right and left peroneal vein as well as right and left posterior tibial vein, the circle represents the gastrocnemius muscle (see *Figures S1,S2*). (Bottom) At the level of the knee: popliteal vein (arrow) and gastrocnemius medial head muscle (circle, see *Figures S3,S4*). PC, phase-contrast.

The results for a patient with DVT are shown in *Figures 4* and *5*. Although flow in the popliteal artery and saphenous vein are clearly seen in both the magnitude image and PC velocity map (*Figure 4*), the popliteal vein is poorly identified due to very low flow caused by thrombus blockage in the vessel. During foot flapping, which was only possible for a few seconds as indicated by increased through-plane velocity and signal changes during the initial phase, the popliteal vein revealed no significant increase in blood flow velocity (*Figure 5*). In contrast, the observation of a moderate increase of flow in the saphenous vein seems to indicate a compensatory mechanism of venous flow in response to thrombosis of the popliteal vein. However, flow in the saphenous vein turned out to be complex and spatially heterogeneous

which may affect the quantitative analysis.

Discussion

Real-time PC MRI was successfully applied to dynamically monitor exercise-related changes of blood flow in the deep veins of the lower leg. A spatial resolution of 0.5 mm allowed for a proper delineation and segmentation of small blood vessels. Because muscular activity was employed as the primary driving force for flow in this study, a temporal resolution of 100 ms was fully sufficient to account for respective changes in flow.

Previous studies of the veins of the limbs (30-32) reported a modulation of venous flow by respiration. In contrast, the present findings clearly demonstrate that

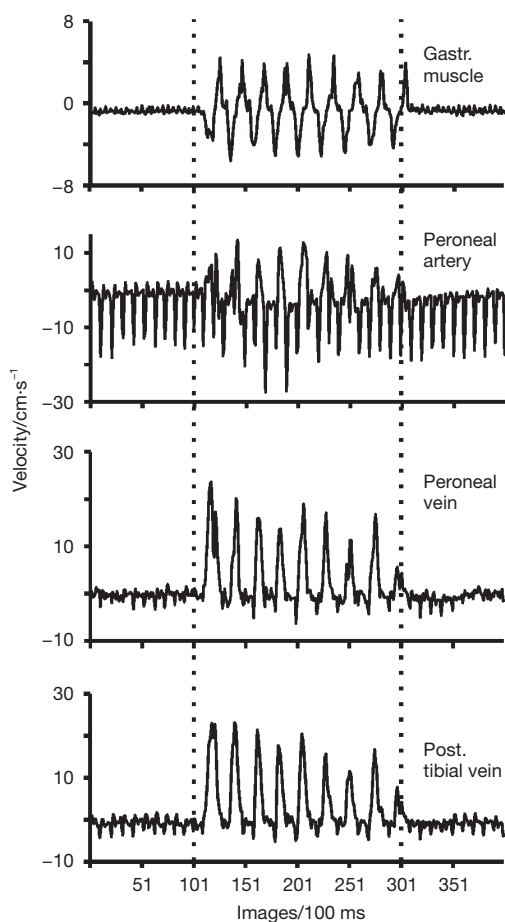


Figure 2 Mean velocities of gastrocnemius muscle, peroneal artery, right peroneal vein, and right posterior tibial vein at the level of the calf muscle (subject #5) for 10 s of rest, 20 s foot flapping, and 10 s rest at 100 ms resolution.

flow in the deep veins of the lower leg is very small and mainly driven by arterial pulsation during resting phases with normal breathing, while much higher venous return from the lower limbs to the heart occurs during muscle movements such as foot flapping. This latter observation confirms the results of a respiration-synchronized PC flow MRI study (31), which reported flow velocities of 15 to 19 $\text{cm}\cdot\text{s}^{-1}$ in the popliteal vein during mild calf exercise in excellent agreement with the values reported in *Table 1*.

Though the influence of exercise on arterial supply to the lower leg was not in the focus of this work, the data for the peroneal artery suggests that both arterial flow velocity and direction are affected by the strength and direction of muscular movements. In general, flow (i.e., velocity and volume) in the popliteal vein at the lower knee was found

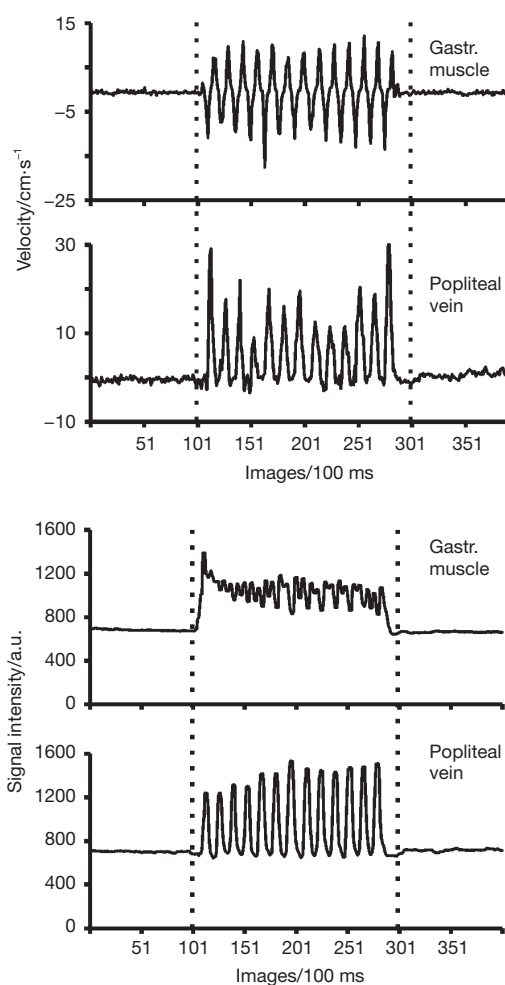


Figure 3 (Top) mean velocities and (Bottom) signal intensities of gastrocnemius medial head muscle and popliteal vein at the level of the knee (subject #2) for 10 s of rest, 20 s foot flapping, and 10 s rest at 100 ms resolution.

to be much higher than in the deep veins at the level of the calf muscle. Flow volumes not only reflect the mean (or integrated) velocity across the vessel lumen, but also the effective size of the lumen during flow. For the present subjects these values differed between calf veins and the popliteal vein by almost a factor of 4. The remaining difference must be ascribed to the facilitated flow in a larger vessel where border zones have less influence. These conditions yield a twofold higher mean velocity (*Table 1*) and most likely lead to a much more effective laminar (i.e., parabolic) flow profile across the lumen.

Movements of the muscles involved in foot flapping were not analyzed in detail, although the velocities of the

Table 1 Mean maximal velocities in deep veins during muscle movement

Subject	Mean maximal velocity/cm·s ⁻¹ (mean ± SD)		
	Peroneal vein	Posterior tibial vein	Popliteal vein
#1	6.2±1.8	6.0±2.3	21.8±3.7
#2	7.8±2.8	7.6±2.0	18.3±6.5
#3	17.9±6.3	12.1±5.3	19.2±5.3
#4	8.9±2.5	9.2±4.2	4.8±2.1
#5	17.2±3.6	17.5±5.2	19.7±7.3
#6	10.6±10.5	4.4±2.2	17±7.9
#7	3.2±2.3	3.2±2.3	17.3±6.9
#8	3.3±1.1	8.0±3.4	24.6±6.2
Mean ± SD	9.4±5.7	8.5±4.6	17.8±5.8

SD, standard deviation.

Table 2 Net flow volume in deep veins during muscle movement

Subject	Net flow volume/mL ¹		
	Peroneal vein	Posterior tibial vein	Popliteal vein
#1	3.2	1.7	53.3
#2	0.0	-0.6	41.4
#3	2.7	1.5	68.9
#4	1.4	0.6	9.4
#5	6.8	7.6	75.7
#6	1.7	-0.5	58.0
#7	0.0	1.1	58.0
#8	-0.7	1.5	33.3
Mean ± SD	1.9±2.4	1.6±2.6	50±21

¹, summed response to multiple foot flaps during 20 s of exercise. SD, standard deviation.

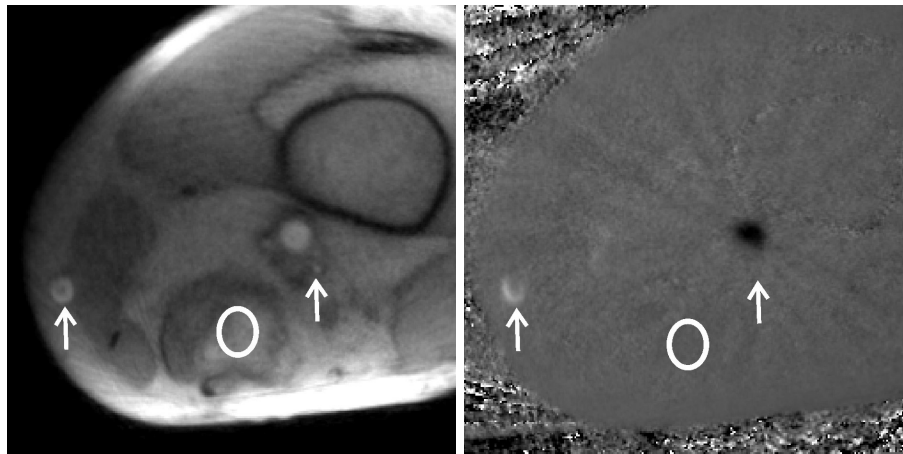


Figure 4 Selected real-time T1-weighted image and PC map of deep venous flow of a patient with DVT at the level of the knee. Arrows refer to (left) saphenous vein and (right) popliteal vein, the circle represents the gastrocnemius medial head muscle. PC, phase-contrast; DVT, deep-vein thrombosis.

gastrocnemius muscle for all subjects were in the range of 10 to $-10 \text{ cm}\cdot\text{s}^{-1}$ for flexion and extension. In future studies it may be considered to directly correlate venous flow and muscular involvement in the lower leg.

While quantitative flow studies are best accomplished by analyzing PC velocity maps, signal intensities in corresponding magnitude images provide qualitative diagnostic information of enhanced sensitivity as exploited in a real-time MRI study of cerebrospinal fluid flow (26).

Such complementary data without the need for another measurement may turn out to be useful for studies of patients with DVT who are either unable to perform suitable muscle movements or suffer from severe thrombosis with little or no venous flow. In fact, this situation holds true for a DVT patient where the intensities in the popliteal vein in response to exercise offered a better contrast-to-noise ratio for the assessment of residual flow than the corresponding velocities.

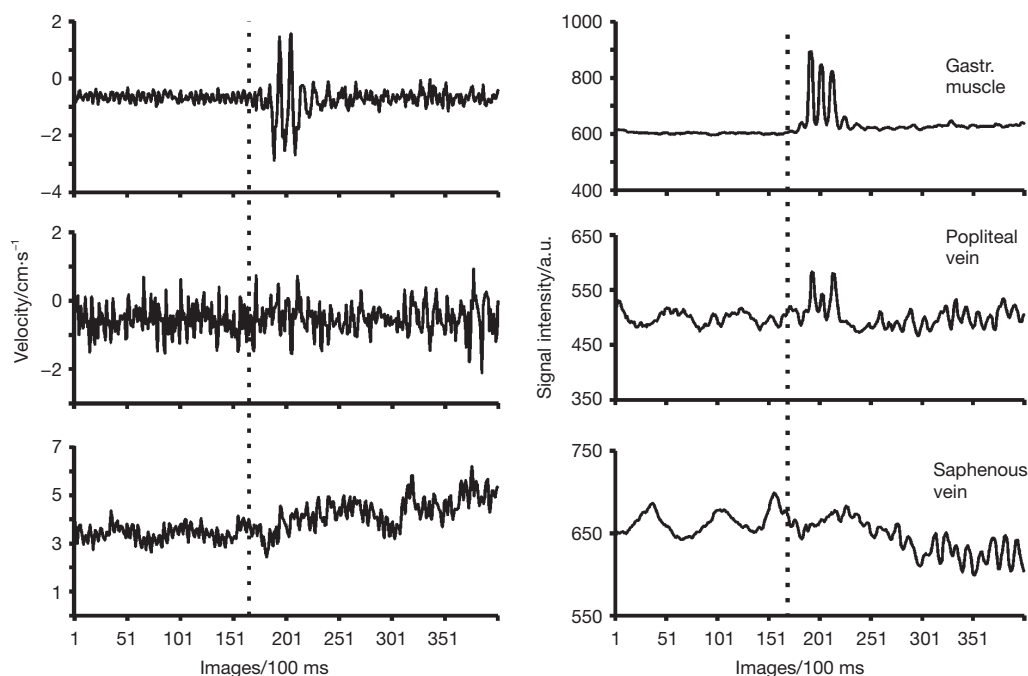


Figure 5 (Left) Mean velocities and (right) signal intensities of gastrocnemius medial head muscle, popliteal vein and saphenous vein in a patient with DVT of the popliteal vein at the level of the knee (16 s rest followed by foot flapping, 100 ms resolution). The results for the saphenous vein are affected by the occurrence of a complex flow pattern (see *Figures S5,S6*). DVT, deep-vein thrombosis.

As this work represents a pilot study of blood flow in peripheral veins, it has limitations due to a small sample size and the lack of reproducibility tests. On the other hand, the actual real-time MRI method and its extension to PC flow imaging have extensively been validated in previous publications dealing with the actual technology, experimental flow phantoms, and aortic blood flow in healthy subjects (21-24). Another potential confound arises from interindividual differences in muscular performance with respect to amplitude, speed and frequency of foot flapping. Although a direct correlation with the actual muscular involvement might be possible by using the simultaneous velocity information for specific muscle groups, this was beyond the scope of this proof-of-concept study. Finally, residual streaking artifacts in PC velocity maps may appear around high-flow arteries and eventually affect the phase information in neighboring veins. While no major complication was observed in the present study, the problem may be resolved by a more advanced reconstruction technique for real-time PC flow MRI which almost completely avoids such artifacts (33).

In conclusion, real-time PC MRI offers a fast and robust tool for simultaneously measuring cardiac-driven arterial flow

and muscle-induced flow in all peripheral veins. The approach may become of clinical value in a variety of disorders such as varicose veins, post-thrombotic syndrome and DVT as the major cause of life-threatening pulmonary thromboembolism. Although ultrasound of blood flow in proximal veins such as the saphenous vein is the current standard for examination of thrombosis in the lower leg, MRI may be beneficial in cases of ultrasound failure (e.g., difficult DVT locations) or in the quantitative assessment of reflow after successful recanalization by pharmacologic or mechanic thrombolysis. Real-time PC MRI of deep veins therefore awaits clinical trials of larger cohorts of patients to ascertain its sensitivity and specificity for the assessment of compromised venous return.

Acknowledgements

AA Joseph received financial support by the DZHK (German Center for Cardiovascular Research) and by the BMBF (German Ministry of Education and Research).

Footnote

Conflicts of Interest: J Frahm is co-inventor of a patent

covering the real-time MRI technique used in this study. The other authors have no conflicts of interest to declare.

Ethical Statement: All participants were recruited after ethics approval by the institutional review board of the University Medical Center Göttingen (approval number: 11/9/11). All participants gave written informed consent before MRI.

References

- Anderson FA Jr, Wheeler HB, Goldberg RJ, et al. A population-based perspective of the hospital incidence and case-fatality rates of deep vein thrombosis and pulmonary embolism. The Worcester DVT Study. *Arch Intern Med* 1991;151:933-8.
- Prandoni P, Lensing AW, Cogo A, et al. The long-term clinical course of acute deep venous thrombosis. *Ann Intern Med* 1996;125:1-7.
- Hansson PO, Welin L, Tibblin G, et al. Deep vein thrombosis and pulmonary embolism in the general population. 'The Study of Men Born in 1913'. *Arch Intern Med* 1997;157:1665-70.
- Agnelli G, Ranucci V, Veschi F, et al. Clinical outcome of orthopaedic patients with negative lower limb venography at discharge. *Thromb Haemost* 1995;74:1042-4.
- White RH, McGahan JP, Daschbach MM, et al. Diagnosis of deep-vein thrombosis using duplex ultrasound. *Ann Intern Med* 1989;111:297-304.
- Lensing AW, Prandoni P, Prins MH, et al. Deep-vein thrombosis. *Lancet* 1999;353:479-85.
- Kearon C, Julian JA, Newman TE, et al. Noninvasive diagnosis of deep venous thrombosis. McMaster Diagnostic Imaging Practice Guidelines Initiative. *Ann Intern Med* 1998;128:663-77.
- Moran PR. A flow velocity zeugmatographic interlace for NMR imaging in humans. *Magn Reson Imaging* 1982;1:197-203.
- van Dijk P. Direct cardiac NMR imaging of heart wall and blood flow velocity. *J Comput Assist Tomogr* 1984;8:429-36.
- Bryant DJ, Payne JA, Firmin DN, et al. Measurement of flow with NMR imaging using a gradient pulse and phase difference technique. *J Comput Assist Tomogr* 1984;8:588-93.
- Sodickson DK, Manning WJ. Simultaneous acquisition of spatial harmonics (SMASH): fast imaging with radiofrequency coil arrays. *Magn Reson Med* 1997;38:591-603.
- Pruessmann KP, Weiger M, Scheidegger MB, et al. SENSE: sensitivity encoding for fast MRI. *Magn Reson Med* 1999;42:952-62.
- Rasche V, de Boer RW, Holz D, et al. Continuous radial data acquisition for dynamic MRI. *Magn Reson Med* 1995;34:754-61.
- Meyer CH, Hu BS, Nishimura DG, et al. Fast spiral coronary artery imaging. *Magn Reson Med* 1992;28:202-13.
- Pelc NJ, Herfkens RJ, Shimakawa A, et al. Phase contrast cine magnetic resonance imaging. *Magn Reson Q* 1991;7:229-54.
- Gatehouse PD, Firmin DN, Collins S, et al. Real time blood flow imaging by spiral scan phase velocity mapping. *Magn Reson Med* 1994;31:504-12.
- Eichenberger AC, Schwitter J, McKinnon GC, et al. Phase-contrast echo-planar MR imaging: real-time quantification of flow and velocity patterns in the thoracic vessels induced by Valsalva's maneuver. *J Magn Reson Imaging* 1995;5:648-55.
- Steeden JA, Atkinson D, Taylor AM, et al. Assessing vascular response to exercise using a combination of real-time spiral phase contrast MR and noninvasive blood pressure measurements. *J Magn Reson Imaging* 2010;31:997-1003.
- Uecker M, Hohage T, Block KT, et al. Image reconstruction by regularized nonlinear inversion--joint estimation of coil sensitivities and image content. *Magn Reson Med* 2008;60:674-82.
- Uecker M, Zhang S, Frahm J. Nonlinear inverse reconstruction for real-time MRI of the human heart using undersampled radial FLASH. *Magn Reson Med* 2010;63:1456-62.
- Uecker M, Zhang S, Voit D, et al. Real-time MRI at a resolution of 20 ms. *NMR Biomed* 2010;23:986-94.
- Joseph AA, Merboldt KD, Voit D, et al. Real-time phase-contrast MRI of cardiovascular blood flow using undersampled radial fast low-angle shot and nonlinear inverse reconstruction. *NMR Biomed* 2012;25:917-24.
- Joseph A, Kowallick JT, Merboldt KD, et al. Real-time flow MRI of the aorta at a resolution of 40 msec. *J Magn Reson Imaging* 2014;40:206-13.
- Untenberger M, Tan Z, Voit D, et al. Advances in real-time phase-contrast flow MRI using asymmetric radial gradient echoes. *Magn Reson Med* 2016;75:1901-8.
- Zhang S, Joseph AA, Gross L, et al. Diagnosis of Gastroesophageal Reflux Disease Using Real-time Magnetic Resonance Imaging. *Sci Rep* 2015;5:12112.
- Dreha-Kulaczewski S, Joseph AA, Merboldt KD, et al.

- Inspiration is the major regulator of human CSF flow. *J Neurosci* 2015;35:2485-91.
27. Zhang S, Joseph AA, Voit D, et al. Real-time magnetic resonance imaging of cardiac function and flow-recent progress. *Quant Imaging Med Surg* 2014;4:313-29.
 28. Schaetz S, Uecker M. A Multi-GPU Programming Library for Real-Time Applications. In: *Lect Notes Comp Sci* 7439, Springer: Berlin Heidelberg, 2012:114-28.
 29. Chitiboi T, Hennemuth A, Tautz L, et al. Context-based segmentation and analysis of multi-cycle real-time cardiac MRI. *IEEE Int Symp Biomed Imaging* 2014:943-6.
 30. Willeput R, Rondeux C, De Troyer A. Breathing affects venous return from legs in humans. *J Appl Physiol Respir Environ Exerc Physiol* 1984;57:971-6.
 31. Miller JD, Pegelow DF, Jacques AJ, et al. Skeletal muscle pump versus respiratory muscle pump: modulation of venous return from the locomotor limb in humans. *J Physiol* 2005;563:925-43.
 32. Pierce IT, Gatehouse PD, Xu XY, et al. MR phase-contrast velocity mapping methods for measuring venous blood velocity in the deep veins of the calf. *J Magn Reson Imaging* 2011;34:634-44.
 33. Tan Z, Roeloffs V, Voit D, et al. Model-based reconstruction for real-time phase-contrast flow MRI: Improved spatiotemporal accuracy. *Magn Reson Med* 2016. [Epub ahead of print].

Cite this article as: Joseph AA, Merboldt KD, Voit D, Dahm J, Frahm J. Real-time magnetic resonance imaging of deep venous flow during muscular exercise—preliminary experience. *Cardiovasc Diagn Ther* 2016;6(6):473-481. doi: 10.21037/cdt.2016.11.02



Figure S1 Real-time MRI movie of T1-weighted images of a healthy subject (calf muscle) during 10 s rest, 20 s foot flapping, and 10 s rest (400 frames at 10 fps) (34). MRI, magnetic resonance imaging. Available online: <http://www.asvide.com/articles/1298>



Figure S4 Real-time MRI movie of PC maps of a healthy subject (knee) corresponding to *Figure S3* (37). MRI, magnetic resonance imaging; PC, phase-contrast. Available online: <http://www.asvide.com/articles/1301>



Figure S2 Real-time MRI movie of PC maps of a healthy subject (calf muscle) corresponding to *Figure S1* (35). MRI, magnetic resonance imaging; PC, phase-contrast. Available online: <http://www.asvide.com/articles/1299>



Figure S5 Real-time MRI movie of T1-weighted images of a patient with DVT (knee) during 16 s rest followed by foot flapping (400 frames at 10 fps) (38). MRI, magnetic resonance imaging; DVT, deep-vein thrombosis. Available online: <http://www.asvide.com/articles/1302>



Figure S3 Real-time MRI movie of T1-weighted images of a healthy subject (knee) as in *Figure S1* (36). MRI, magnetic resonance imaging. Available online: <http://www.asvide.com/articles/1300>



Figure S6 Real-time MRI movie of PC maps of patient with DVT (knee) corresponding to *Figure S5* (39). MRI, magnetic resonance imaging; PC, phase-contrast; DVT, deep-vein thrombosis. Available online: <http://www.asvide.com/articles/1303>

References

34. Joseph AA, Merboldt KD, Voit D, et al. Real-time MRI movie of T1-weighted images of a healthy subject (calf muscle) during 10 s rest, 20 s foot flapping, and 10 s rest (400 frames at 10 fps). *Asvide* 2016;3:523. Available online: <http://www.asvide.com/articles/1298>
35. Joseph AA, Merboldt KD, Voit D, et al. Real-time MRI movie of PC maps of a healthy subject (calf muscle) corresponding to Figure S1. *Asvide* 2016;3:524. Available online: <http://www.asvide.com/articles/1299>
36. Joseph AA, Merboldt KD, Voit D, et al. Real-time MRI movie of T1-weighted images of a healthy subject (knee) as in Figure S1. *Asvide* 2016;3:525. <http://www.asvide.com/articles/1300>
37. Joseph AA, Merboldt KD, Voit D, et al. Real-time MRI movie of PC maps of a healthy subject (knee) corresponding to Figure S3. *Asvide* 2016;3:526. Available online: <http://www.asvide.com/articles/1301>
38. Joseph AA, Merboldt KD, Voit D, et al. Real-time MRI movie of T1-weighted images of a patient with DVT (knee) during 16 s rest followed by foot flapping (400 frames at 10 fps). *Asvide* 2016;3:527. Available online: <http://www.asvide.com/articles/1302>
39. Joseph AA, Merboldt KD, Voit D, et al. Real-time MRI movie of PC maps of patient with DVT (knee) corresponding to Figure S5. *Asvide* 2016;3:528. Available online: <http://www.asvide.com/articles/1303>